Hindawi
Journal of Chemistry
Volume 2022, Article ID 1241470, 15 pages
https://doi.org/10.1155/2022/1241470

Research Article

Synthesis, Characterization, X-Ray Single-Crystal Structure, Potentiometric Measurements, Molecular Modeling, and Bioactivity Screening of Some Thiosemicarbazones

Abeer A. El-Sisi,[1] Mohamed Ali,[1] Sohair F. Ramdan,[2] Osama AlTaweel,[3] Ahmed I. A. Abd El-Mageed,[4,5] and Ahmed A. El-Sherif[1]

[1]*Department of Chemistry, Faculty of Science, Cairo University, Cairo, Egypt*
[2]*Department of Zoology, Faculty of Science, Cairo University, Cairo, Egypt*
[3]*Department of Forensic Medicine, Faculty of Veterinary, Cairo University, Cairo, Egypt*
[4]*Chemistry Department, Faculty of Science, Galala University, Galala City, Suez 43711, Egypt*
[5]*Chemistry Department, Faculty of Science, Minia University, Minia 61519, Egypt*

Correspondence should be addressed to Ahmed A. El-Sherif; aelsherif72@yahoo.com

Received 24 July 2021; Revised 8 January 2022; Accepted 23 March 2022; Published 9 July 2022

Academic Editor: Josefina Pons

A series of thiosemicarbazone (TSCN) compounds including ((E)-2-((E)-1-(2-(p-tolyl)hydrazono)propan-2-ylidene)hydrazine-1-carbothioamide (TSC1), (E)-N-ethyl-2-((E)-1-(2-(p-tolyl)hydrazono)propan-2-ylidene)hydrazine-1-carbothioamide (TSC2), and (E)-N-phenyl-2-((E)-1-(2-(p-tolyl)hydrazono)propan-2-ylidene)hydrazine-1-carbothioamide) (TSC3) were synthesized and fully characterized by diverse spectroscopies, such as X-ray single-crystal, infrared, mass, proton nuclear magnetic resonance, and ultraviolet-visible. Potentiometric measurements, molecular modeling, and biological and antitumor activity screening were studied. The thermodynamics and protonation constants of TSC1 as a representative of the synthesized TSCs were calculated and discussed. The solution speciation of different species was studied with pH. The molecular parameters of the optimized structures were calculated and discussed. The X-ray single crystals of TSC2 and TSC3 were established. Considering the antimicrobial activities and correlating structure-activity relationship of the synthesized compounds, the TSC1 molecule was considered a promising candidate as an antifungal agent against *Candida albicans*. Thus, it would be extremely helpful in the field of medicinal chemistry, particularly as an antimicrobial agent. The results are of significance to the chemistry of antimicrobial agents.

1. Introduction

Globally, infectious diseases constitute a high burden on public health worldwide. Owing to the high resistance of certain Gram-positive and Gram-negative bacteria to many drugs, a large number of infectious diseases threaten human life worldwide [1]. Globally, approximately 110000 of over 50 million infected people die annually. By the middle of the 21st century, it is expected that the mortality rate caused by Gram-negative bacterial infection alone could increase to 10 million deaths annually [2]. Antibiotics are the main base for microbial (bacterial and fungal) infection therapy. Antibiotic overuse has become the main cause of the appearance and spread of multidrug-resistant strains of many microbes [3]. The emergence and increasing prevalence of antibiotic-resistant bacterial strains urge the discovery of new therapeutic approaches [4]. Additionally, the available drugs are expensive or exhibit many unwanted side effects [5]. Therefore, the development of novel antimicrobial agents is vital, given the fast global spread of resistant clinical isolates. Considering the relationship between bacterial infection and multidrug resistance, this study developed a new effective

antimicrobial drug. Nowadays, there is a growing area of interest in the medicinal chemistry of Schiff base compounds, such as hydrazones and thiosemicarbazones (TSCs), owing to their wide range of biological activities [6, 7]. C=N and N–C = S groups are of great interest in chemotherapy and are responsible for the pharmacological activity therein. The most essential step in the metal complex implementation is the synthesis of novel compounds that exhibit unique properties and reactivity. In this regard, TSCs are a topic of interest for researchers of various profiles. TSCN compounds and their complexes have been widely investigated as they exhibit extremely interesting properties for biomedicine and potential medicinal applications [8–12]. These properties comprise antiparasitic [13], antibacterial [14], antitumor [15], antiviral [16], fungicidal [17], antineoplastic [18], and antiamebic [19] activities. TSCs exhibit thione (A) and thiol (B) forms (Scheme 1).

Hydrazones are a crucial class of compounds with impressive ligation characteristics, owing to the existence of several coordination sites [20]. Previous reports show hydrazine and its derivatives with anti-inflammatory, analgesic [21], antibacterial [22], and antitumor [23] activity.

Cd is an extremely toxic metal ion that poses human and animal health hazards. Its toxicity is caused by its easy localization inside the liver. It binds to metallothionein, which eventually forms a complex and is transmitted into the bloodstream to be lodged in the kidney.

Cd toxicity is caused by the negative effect on cell enzyme systems that are the consequence of metallic ion substitution (mainly Zn (II), Cu (II), and Ca (II)) into metalloenzymes and their large affinity to thiol group compounds [24]. Zn (II) replacement with a chemically analogous Cd (II) ion usually causes apoprotein catalytic activity to break down [25, 26]. Therefore, it is important to discover novel compounds that can form stable complexes with Cd (II) because they can be used as detoxifiers. TSCN compounds and their complexes are fit for this role because of their pharmacological properties. Recently, experimental studies were supplemented by computational studies [27], owing to their crucial role in recognizing the expected behaviors of the compound during reactions and recognition of valuable information on the compounds under examination, such as the total energy, binding energy, electronic energy, dipole moment, bond length, highest occupied molecular orbital (HOMO), and lowest unoccupied molecular orbital (LUMO) [28–30]. Based on this and in the perpetuation of our studies in the subject area of bioactive compounds, it is of great interest to synthesize and identify novel compounds with TSCN and hydrazone moieties. In addition, we explored the biological activities of the identified compounds.

2. Experimental Process

2.1. Materials and Reagents. The chemicals used in this study were supplied by Aldrich Chemicals Company and were used without extra purification.

2.2. Synthesis

2.2.1. Synthesis of (1-(p-Tolyl)Hydrazono)Propan-2-One (PTHP). We synthesized PTHP using a reported method [31, 32]. Scheme 2 shows the chemical equations for the preparation.

$$\begin{aligned} CH_3COCH_2CO_2C_2H_5 + KOH &\longrightarrow CH_3COCH_2CO_2K + C_2H_5OH, \\ CH_3COCH_2CO_2K + HCl &\longrightarrow CH_3COCH_2CO_2H + , \\ CH_3COCH_2CO_2H + p - Me - C_6H_5N = NCl &\longrightarrow p - Me - C_6H_5NH - N = CHCOCH_3 + CO_2 + HCl. \end{aligned} \quad (1)$$

2.2.2. Synthesis of TSCN Compounds. Equimolar amounts of PTHP (0.1760 g, 1 mmol) in 30 mL of ethanol with an ethanolic solution (30 mL) of thiosemicarbazide (0.091 g, 1 mmol), N-ethylthiosemicarbazide (0.119 g, 1 mmol), and N-phenylthiosemicarbazide (0.167 g, 1 mmol) were refluxed on a hot plate for 3–5 hrs. The precipitate was separated, filtered off, washed with $(C_2H_5)_2O$, and desiccated all night using silica gel. The target compounds are shown in Figure 1.

(1) ((E)-2-((E)-1-(2-(p-Tolyl)Hydrazono)Propan-2-Ylidene) Hydrazine-1-Carbothioamide (TSC1). Yield, 77%. Color, brown. Anal. Calc. for $C_{11}H_{15}N_5S$: C, 52.99; H, 6.06; N, 28.09; S, 12.86. Found: C, 52.93; H, 6.01; N, 28.03; S, 12.79%. Infrared (IR) (KBr, cm^{-1}): 3386, 3234 (NH_2), 1507, 1251, 1017, 805 (thioamide bands, I–IV, respectively), 3501, 3177 (N2H), 1100 (N–N), 1603 (C = N), 1553 (C = C), 3045 (C–H). MS (m/z): 251 (M^++2, 6.03%), 250 (M^++1, 18.07%), 249 (M^+, 100%), 234 (2.58%), 232 (38.20%), 159 (2.07%), 157 (0.59%), 118 (3.81%). Proton nuclear magnetic resonance (^{1}H NMR) (DMSO): 11.32 (s, 1H, NH); 10.89 (s, 2H, NH); 7.8 (s, 2H, NH_2); 7.48 (s, H, CH = N); 6.94–7.01 (m, 4H,–Ar); 2.21 (s, 3H,–CH_3); 2.02 (s, 3H,–CH_3). ^{13}C-NMR (DMSO): 11.02, 20.09, 112.21, 129.51, 130.80, 136.01, 142.21, 145.62, 178.3.

(2) ((E)-N-Ethyl-2-((E)-1-(2-(p-Tolyl)Hydrazono)Propan-2-Ylidene)Hydrazine-1-Carbothioamide (TSC2). Yield, 69%. Color, dark brown. Anal. Calc. for $C_{13}H_{19}N_5S$: C, 55.52; H, 6.17; N, 25.25; S, 11.56. Found: C, 55.48; H, 6.12; N, 25.19; S, 11.51%. IR (KBr, cm^{-1}): 1532, 1251, 1079, 805 (thioamide bands, I–IV, respectively), 3444, 3338, 3230 (3NH), 1079 (N–N), 1615 (C = N), 1535 (C = C), 3019 (C–H). MS (m/z): 279 (M^++2, 6.53%), 278 (M^++1, 21.11%), 277 (M^+, 100%), 262 (0.94%), 173 (2.73%), 118 (3.23%). ^{1}H-NMR: 11.33 (s, 1H, NH); 10.33 (s, 1H, NH); 8.91 (s, 1H, NH); 7.54 (s, H, CH = N); 6.36–7.54 (m, 4H,–Ar); 3.60 (q, 2H,–CH_2); 2.4 (t,

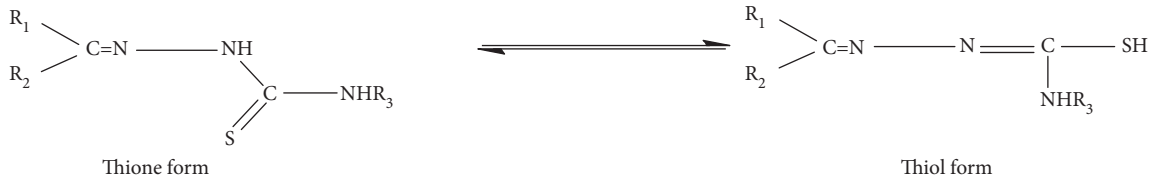

Scheme 1: Thione (a) and thiol (b) tautomers of thiosemicarbazones.

$CH_3COCH_2CO_2C_2H_5 + KOH \rightarrow CH_3COCH_2CO_2K + C_2H_5OH,$
$CH_3COCH_2CO_2K + HCl \rightarrow CH_3COCH_2CO_2H + KCl,$
$CH_3COCH_2CO_2H + p\text{-}Me\text{-}C_6H_5N{=}NCl \rightarrow p\text{-}Me\text{-}C_6H_5NH\text{-}N{=}CHCOCH_3 + CO_2 + HCl.$

Scheme 2: Preparation of (1-(p-tolyl)hydrazono)propan-2-one.

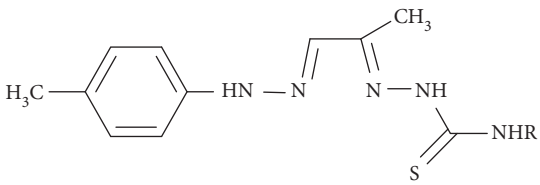

Figure 1: Structural formula for the thiosemicarbazone compounds. TSC1, TSC2, and TSC3 with R = H, Et, and ph, respectively.

2H,–CH_3); 2.23 (s, 3H,–CH_3); 2.02 (s, 3H,–CH_3). ^{13}C-NMR: 11.01, 14.32, 20.09, 39.21, 112.23, 128.07, 129.61, 136.0, 142.23, 148.24, 177.04.

(3) (E)-N-Phenyl-2-((E)-1-(2-(p-Tolyl)Hydrazono)Propan-2-Ylidene)Hydrazine-1-Carbothioamide (TSC3). Yield, 67%. Color, brownish yellow. Anal. Calc. for $C_{17}H_{19}N_5S$: C, 62.74; H, 5.89; N, 21.50; S, 9.85. Found: C, 62.75; H, 5.85; N, 21.47; S, 9.81%. IR (KBr, cm^{-1}): 1518, 1250, 1065, 748 (thioamide bands, I–IV, respectively), 3444, 3259, 3020 (3NH), 1065 (N–N), 1603 (C = N), 1551 (C = C), 3020 (C–H). MS (m/z): 326 (M^++1, 1.78%), 325 (M^+, 7.41%), 118 (5.63%). ^{1}H-NMR: 11.32 (s, 1H, NH); 10.30 (s, H, NH); 7.70 (s, H, NH); 7.61 (s, H, CH = N); 6.4–7.70 (m, 9H,–Ar); 2.21 (s, 3H,–CH_3); 2.03 (s, 3H,–CH_3). ^{13}C-NMR: 11.33, 20.13, 39.40, 112.24, 115.63, 124.94, 128.28, 129.47, 135.87, 138.92, 142.16, 149.22, 175.9.

2.3. Methods and Experimental Measurements. The chemicals used were supplied by Aldrich. A CHNS automatic analyzer (Vario EII-Elementar) was used to conduct elemental microanalysis for C, H, N, and S. A PerkinElmer Fourier transform IR (FTIR) type 1650 spectrophotometer with a potassium bromide disc was used to record the IR spectra. Electronic spectra were recorded on a Shimadzu UV-3101PC spectrophotometer. A Bruker ARX-300 device was applied to record the ^{1}H-NMR spectra. Chemical shifts were recorded in ppm comparative to tetramethylsilane (TMS) using deuterated dimethyl sulphoxide (d_6-DMSO) as a solvent. Mass spectrometry was conducted using a Shimadzu GCMS-QP1000EX. The X-ray single-crystal diffraction of the TSC2 molecule was performed using a Rigaku VariMax RAPID FR-E diffractometer with monochromatized Mo Kα radiation at a radiation wavelength of $\lambda = 0.71075$ Å in ω scan mode. The crystal was cooled with a cold N_2 gas flow. We performed diffraction data scaling, cell refinement, indexing, collection, and peak integration using the Rapid Auto software (Rigaku). The molecular structure was analyzed using Mercury 4.1.3 software. However, the X-ray crystallography data of TSC2 and TSC3 were collected by mounting a single sample crystal on glass fiber. The cell parameters and intensity data collection were performed at 298 K using monochromatized Mo Kα radiation at a radiation wavelength of $\lambda = 0.71073$ Å. The crystal structure was analyzed using the SIR-92 program [33] and was refined on F^2 using the full-matrix least-squares technique with the maXus processor program for the solution and refinement of crystal structures [34]. The Oak Ridge Thermal Ellipsoid Plot (ORTEP) program was used for molecular graphics [35].

A Metrohm 848 Titrino supplied with a Dosimat unit (Switzerland-Herisau) was used for potentiometric titrations as previously described in 50% water-DMSO mixture [29, 30, 32].

2.4. Potentiometric Titrations. Using the aforementioned potentiometric technique [36], the formation constant of the complex was estimated. Standard buffer solutions were used to accurately calibrate the glass electrode to the National Bureau of Standards (NBS) [37]. A standard solution of 0.05 mol/dm^3 NaOH, free from CO_2, was used to titrate the samples in an N_2 atmosphere. The sample solution was developed to avoid hydrolysis during titration by mixing equal volumes of DMSO and H_2O. The ionic strength was maintained during titration using $NaNO_3$ as a supporting electrolyte.

The calculation of the formation constants using the potentiometric method was performed using a concentration of hydrogen ion expressed in molarity. The concentration in the pH meter was expressed in activity coefficient $-\log a_{H+}$ (pH). Thus, Van Uitert and Hass used equation (2) to change the pH meter reading (B) to $[H^+]$ as follows [38, 39]:

$$-\log_{10}[H^+] = B + \log_{10} U_H, \quad (2)$$

where $\log_{10} U_H$ = solvent composition correction factor and the ionic strength read by B. The pK_w values for the titrated samples were estimated as previously described [40]. All precautions and procedures comply with literature requirements [41–43].

The protonation constants of TSC1 were estimated potentiometrically by titrating 40 cm^3 of a 1.25×10^{-3} mol/dm^3 TSC1 solution with a standard sodium hydroxide solution.

2.5. Processing of Data. The MINIQUAD-75 computer program was applied to calculate ca. 100–150 readings for each titration [44]. Species distribution diagrams for the studied samples were produced using the SPECIES program [45].

2.6. Molecular Modeling Studies. Density functional theory (DFT) calculations were performed using the $DMol^3$ program [46, 47] in the Materials Studio package [48]. The calculations for the DFT semicore pseudopods (DSPP) were created with dual numerical base sets and polarization properties (DNPs) [49]. The revised Perdew–Burke–Ernzerhof (RPBE) model was focused on the generalized gradient approximation (GGA) as the best functional approximation [50, 51].

2.7. Biological Activity

2.7.1. Antibacterial and Antifungal Activities. The ability of the synthesized TSCN compounds to suppress bacterial growth was confirmed using the disc diffusion process [52, 53]. Aerobic G^+ bacteria including *Staphylococcus aureus*, *Bacillus subtilis,* and *Streptococcus faecalis* and G^- aerobic bacteria including *Pseudomonas aeruginosa, E. coli,* and *Neisseria gonorrhoeae* were among the bacterial strains used in this study. Additionally, two fungal strains *(Aspergillus flavus* and *Candida albicans)* were confirmed. The stock novel compound solutions were prepared in DMSO. First, 100 μL of each of the synthesized TSCN compounds was inserted into discs (0.8 cm) and allowed to dry. The discs were completely saturated with the synthesized compounds and placed in the upper layer of the medium at least 25 mm from the edge. They were gently placed on the same plate surface. The plate was incubated at 37°C for 72 h, and a clear inhibition area was confirmed. Eventually, using the ruler millimeter, we determined the inhibition zone (an area where there is no growth around the discs).

2.7.2. In Vitro Antitumor Activity. The synthesized TSCN compounds were screened for their cytotoxicity against liver cancer (HepG2) and breast cancer (MCF-7) cells using the sulforhodamine B (SRB) assay protocol [54].

The potential cytotoxicity of the compounds was tested using the method reported by Skehan and Storeng. The cells were plated in 96-multiwell plates (104 cells/well) for 24 h before treatment with the compounds to allow the attachment of the cell to the wall of the plate. Different concentrations of the compounds under investigation (0, 5, 25, and 50 μg/mL) were added to the cell monolayer, and triplicate wells were prepared for each dose. The monolayer cells were incubated with the compounds for 48 h at 37°C in a 5% CO_2 atmosphere. Afterward, the cells were fixed, washed, and stained with SRB. The excess stain was washed with acetic acid, and the attached stain was recovered with tris-ethylenediaminetetraacetic acid (EDTA) buffer. The optical density (OD) of each well was measured spectrophotometrically at 564 nm with an ELISA microplate reader. The mean background absorbance was automatically subtracted, and the mean values of each drug concentration were calculated. The relationship between the drug concentration and surviving fraction was plotted to obtain the survival curve of the breast and liver tumor cell lines for each compound.

The percentage of cell survival was calculated as follows. Survival fraction = OD (treated cells)/OD (control cells). The IC_{50} values are the concentrations of the Schiff base ligand (*L*) or complexes required to produce 50% inhibition of cell growth. The experiment was performed thrice.

3. Results and Discussion

3.1. Characterization of the Synthesized TSCN Compounds. The condensation of PTHP with thiosemicarbazide, N-ethylthiosemicarbazide, and N-phenylthiosemicarbazide readily yielded the corresponding TSC1, TSC2, and TSC3 compounds. The isolated compounds were air-stable and insoluble in H_2O but easily soluble in dimethylformamide (DMF) or DMSO. Different analytical tools were used to identify the structure of the prepared compounds. The results from the basic analysis were correlated with the calculated results for the proposed formula. The novel TSCs structures are shown in Figure 1.

3.1.1. IR Spectrum. The preliminary allocations of major IR spectrum bands of the TSCN compounds showed a disappearance of ν (>C = O) and a new band within the range of 1603–1615 cm^{-1} attributable to ν (C = N) stretching vibration [55], supporting condensation reaction and formation of the TSCN compounds. TSCN compounds exhibit thione ↔ thiol tautomerism [56] because of the existence of an–NH–C = S linkage, but ν (S–H) absorption band within the range of 2500–2600 cm^{-1} was absent with the appearance of ν (C = S) band around 750 cm^{-1}, indicating the existence of the prepared TSCN compounds in the thione form in the solid state. For the prepared TSCN compounds, vibrational bands with the wave numbers of 3012 cm^{-1} (ν_{C-H}, Ar–H), 1615 cm^{-1} ($\nu_{C=N}$), 1548 cm^{-1} ($\nu_{C=C}$), and 1082 cm^{-1} (ν_{N-N}) were detected.

Four vibrational bands with wave numbers in the ranges of 3019–3045 cm^{-1} (ν_{C-H}, Ar–H), 1601–1615 cm^{-1} ($\nu_{C=N}$), 1535–1553 cm^{-1} ($\nu_{C=C}$), and 1065–1100 cm^{-1} (ν_{N-N}) were observed for the TSCN compounds. The ν_{sym} and ν_{asym} of the TSC1 amino group were observed at 3234 and 3386 cm^{-1}, respectively. In the spectra of the TSCN compounds, the bands observed in the ranges of 1494–1532, 1249–1251, 1017–1088, and 748–817 cm^{-1} were assigned to the thioamide bands of I, II, III, and IV, respectively [57].

3.1.2. NMR Spectrum. The ^{1}H-NMR spectra of the novel TSC1, TSC2, and TSC3 compounds in DMSO-d_6 did not exhibit resonance at approximately 4.0 ppm corresponding to the –SH proton resonance [58], whereas the presence of a

peak at 10.77 ppm (signal field of existence of the NH group next to C = S) suggested that they remained in the thione form even in a polar solvent, such as DMSO. The signals for the methine proton of an azomethine group for the TSCN compounds, CH = N, were detected at $\delta = 7.48–7.61$ ppm. In the region of 6.36–7.54 ppm, chemical shifts were allocated for the hydrogen of the aromatic ring. A methyl group was observed as a singlet signal at $\delta = 2.02–2.20$ ppm. The spectrum of TSC1 showed signals at $\delta = 7.80$ ppm, assigned to the NH_2 proton.

The ^{13}C-NMR spectra of the novel TSCN compounds were recorded in DMSO-d6. The peaks of azomethine carbons and C = S of the TSCN compounds were observed as singlet peaks. The signal for the carbon atom of C = S was detected at 178.3, 177.8, and 178.1 in TSC1, TSC2, and TSC3, respectively.

3.1.3. Ultraviolet-Visible (UV-Vis) Spectrum. A strong absorption band detected within the range of 33003–32787 cm^{-1} was assigned to $\pi \longrightarrow \pi^*$ transitions of the $(C = N)_{azomethine}$ group, while the possible assignments for the bands within 26809–27548 cm^{-1} were attributed to $n \longrightarrow \pi^*$TSCN compound transitions. Permanent $\pi \longrightarrow \pi^*$ transitions occur at a higher energy than $n \longrightarrow \pi^*$ transitions [59].

3.1.4. Mass Spectra. The proposed formula was further confirmed by mass spectroscopy. The electron impact mass spectrum of TSC1 confirmed the suggested formula by exhibiting a peak at 249 equivalent to $C_{11}H_{15}N_5S$ compound moiety, in addition to a series of peaks attributable to different fragments of TSC1. These data suggested that a ketone PTHP group was condensed with the NH_2 group of thiosemicarbazide or its derivatives. The mass spectra of TSC1, TSC2, and TSC3 showed peaks at 249, 277, and 325 m/z, confirming the proposed structural formula of the synthesized TSC1, TSC2, and TSC3 compounds, respectively.

3.1.5. Crystallography. The structures of TSC2 and TSC3 were established through X-ray crystallography. The recrystallization of the compounds from hot ethanol, followed by slow evaporation, led to the formation of single crystals. CCDC *2026108 and* CCDC *2033322* contain the supplementary crystallographic data for this study.

The X-ray single-crystal structures of monomeric TSC2 and TSC3 compounds are shown in Figures 2(a) and 2(b), respectively. It suggested that TSC2 was crystallized in a monoclinic crystal system with space $P2_1/c$, $a = 27.985$ (12) Å, $b = 12.027$ (5) Å, $c = 9.833$ (4) Å, $\alpha = 90.0^\circ$, $\beta = 93.117$ (11)°, $\gamma = 90.0^\circ$, V = 3486.57 Å^3, and $Z = 7$, while TSC3 was crystallized also in monoclinic crystal system with space $P2_1/c$, $a = 11.2343$ (6) Å, $b = 11.2575$ (7) Å, $c = 11.8995$ (8) Å, $\alpha = 90.00^\circ$, $\beta = 94.476(6)^\circ$, $\gamma = 90.0^\circ$, V = 1500.34 (3) Å^3, and $Z = 4$.

Note worthily, TSC2 molecules are noncovalently stacked via intermolecular interactions, i.e., van der Waals and H-bonding interactions. This is illustrated in Figure 3. In the packing structure of the TSC2 and TSC3 molecules, the unit cell included four and seven molecules stacked to each other per unit cell.

3.1.6. Molecular Modeling and/or Molecular Parameters. Quantum parameters such as E_{HOMO} and $E_{LUMO,}$ in addition to specific parameters such as the ionization potential (IP), absolute softness (σ), absolute hardness (η), electron affinity (EA), separation energy (ΔE), absolute electronegativity (χ), global softness (S), electrophilicity (w), electron-accepting power (w^+), electron-donating power (w^-), and additional electronic charge (ΔN_{max}) [60–64], have been computed according to Eqs. 2–11 as shown below [60–65]. The inverse of the global hardness is called softness σ [66].

$$\chi = \frac{-1}{2}\left(E_{LUMO} + E_{HOMO}\right), \tag{3}$$

$$IP = -E_{HOMO}, \tag{4}$$

$$\eta = \frac{1}{2}\left(E_{LUMO} - E_{HOMO}\right), \tag{5}$$

$$S = \frac{1}{2\eta}, \tag{6}$$

$$\Delta N_{max} = \frac{-IE}{\eta}, \tag{7}$$

$$\sigma = \frac{1}{\eta}, \tag{8}$$

$$EA = -E_{LUMO}, \tag{9}$$

$$\omega = \frac{IE^2}{2\eta}, \tag{10}$$

$$\omega^- = (3 * IE + EA)\frac{2}{16}(IE - EA), \tag{11}$$

$$\omega^- = (IE + 3 * EA)\frac{2}{16}(IE - EA). \tag{12}$$

The geometric optimization of the prepared compounds can be characterized using theoretical calculations; therefore, the optimized structure for the synthesized compounds was obtained by calculating theoretical physical parameters, such as bond lengths and bond angles using DFT calculations.

The quantum parameters of the synthesized TSC1, TSC2, and TSC3 compounds were calculated using equations (3)–(12). As shown in Tables 1 and 2, we deduced the following:

(a) HOMO and LUMO are frontier molecular orbitals (FMOs). The HOMO and LUMO energies were negative, indicating that the studied TSC1, TSC2, and TSC3 TSCs were stable molecules [65].

(b) The HOMO and LUMO functioned as electron donor and acceptor, respectively [66, 67].

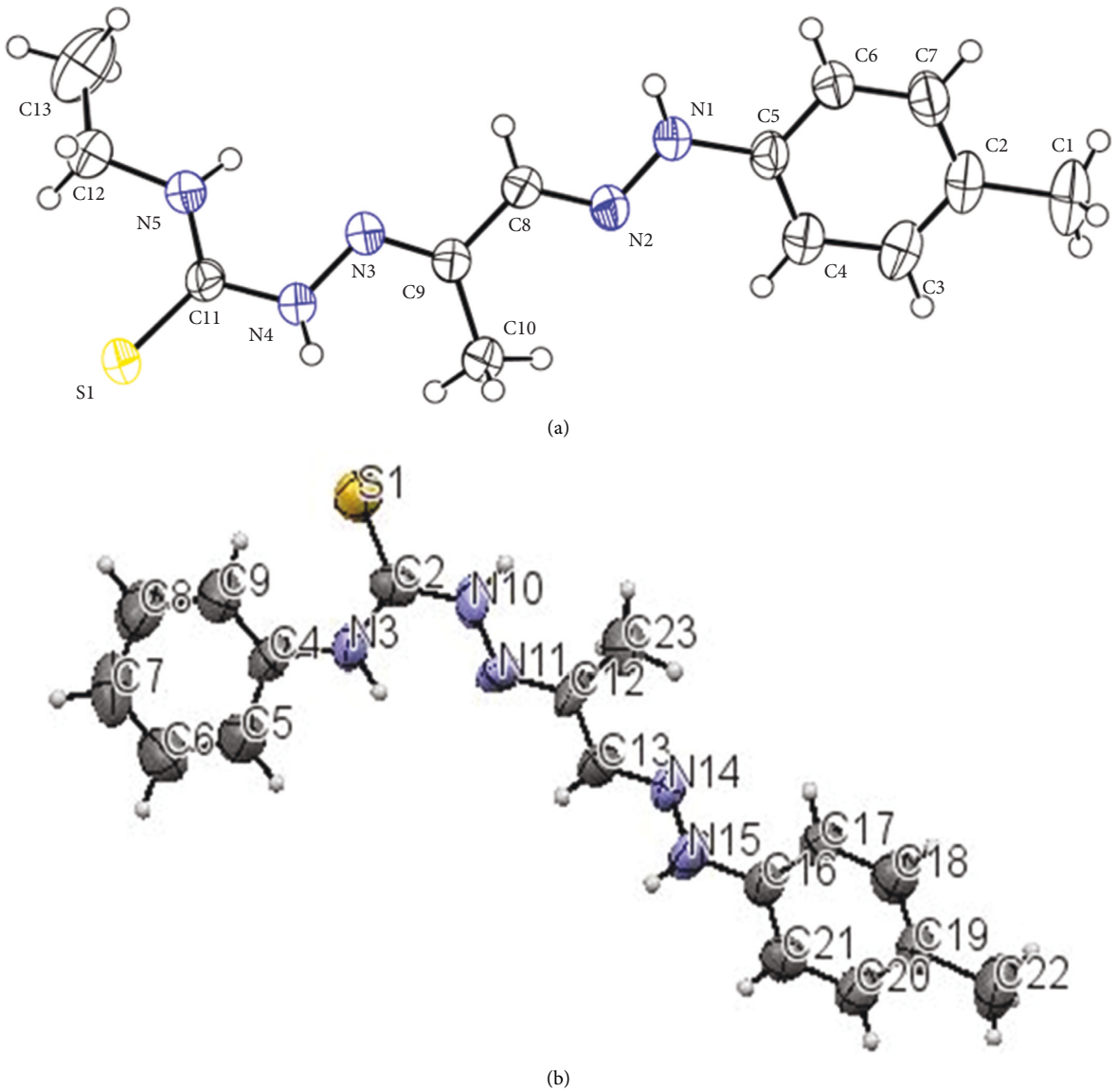

Figure 2: X-ray structure of (a) TSC2 (b) TSC3 along with the atom numbering scheme.

(c) Hard and soft nucleophiles exhibit low and high HOMO energies, respectively, while hard and soft electrophiles exhibit high and low LUMO energies, respectively.

(d) The HOMO energies of TSC1, TSC2, and TSC3 were closely spaced (E_{HOMO} (TSC1) −8.501 eV; E_{HOMO} (TSC2) −8.561 eV; and E_{HOMO} (TSC3) −8.556 eV).

(e) Soft molecules are characterized by a small energy gap (E_{LUMO}–E_{HOMO}) and higher reactivity than hard molecules because of their easy donation of electrons to an acceptor [68, 69].

(f) Large values of the HOMO–LUMO energy gap (7.410–7.667) indicated good stability and a large chemical hardness for the synthesized TSCN compounds.

(g) Absolute hardness (η) and softness (σ) are essential characteristics in the calculation of molecular stability and reactivity. Hard molecules exhibit a large energy gap with less reactivity ($\Delta E = E_{HOMO} - E_{LUMO}$), whereas soft molecules exhibit a smaller energy space and greater reactivity. This indicated that ΔE was an indicator of stability and can be used to measure the chemical reactivity and kinetic stability of the compound [67, 70].

(h) When the HOMO energy decreased, the ability of the molecule to donate electrons decreased, while a high HOMO energy indicated that the molecule was an efficient electron donor. The LUMO energy indicated the ability of a molecule to receive an electron.

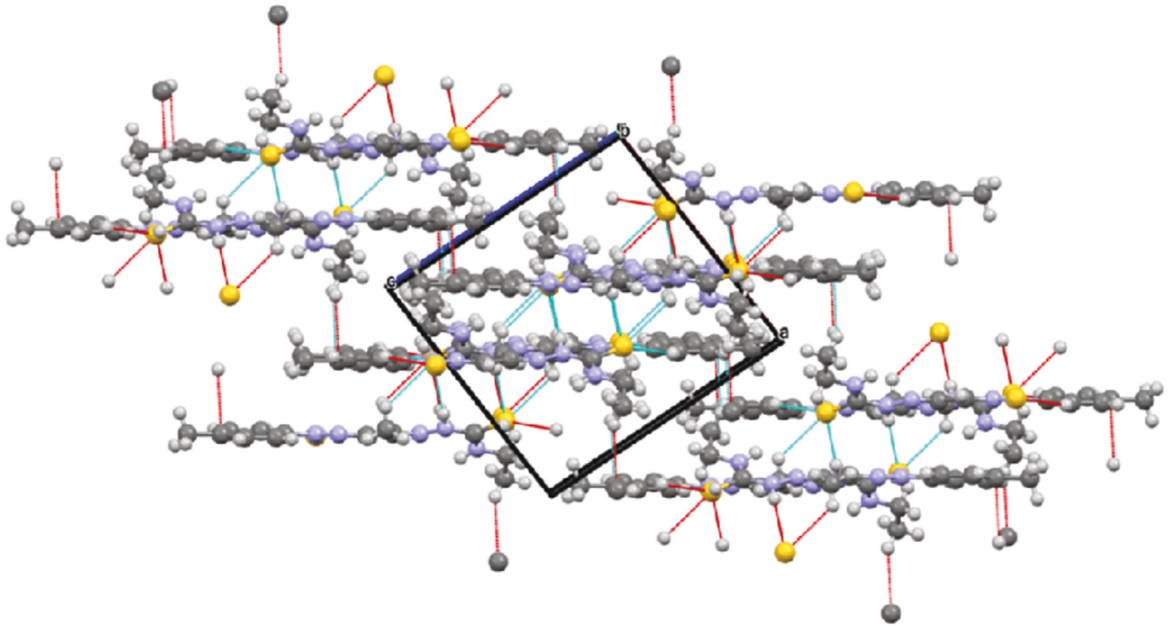

Figure 3: Expansion of the intermolecular interactions (i.e., van der Waals interaction) between the TSC2 molecules.

Table 1: Some energetic properties of the synthesized thiosemicarbazone compounds.

Compound	Total energy (kcal/mol)	Binding energy (kcal/mol)	Electronic energy (kcal/mol)	Dipole moment (Debyes)	HOMO	LUMO
TSC1	−58321.2	−3178.9	−368233.1	6.55	−8.501	−1.091
TSC2	−65214.1	−3735.7	−441527.7	6.82	−8.561	−0.915
TSC3	−79668.2	−4295.6	−566955.2	6.94	−8.556	−0.889

Table 2: Calculated quantum chemical parameters of the synthesized thiosemicarbazone compounds.

Compound	ΔE	I	A	χ	η	S	ΔNmax	ω	$\omega-$	$\omega+$
TSC1	7.410	8.501	1.091	4.796	3.705	0.270	−2.294	3.104	5.965	1.169
TSC2	7.646	8.561	0.915	4.738	3.823	0.262	−2.239	2.936	5.783	1.045
TSC3	7.667	8.556	0.889	4.723	3.834	0.261	−2.232	2.909	5.749	1.027

(i) The electrophilicity index (ω) followed this trend: TSC1 ($\omega = 3.104$) > TSC2 ($\omega = 2.936$) > TSC3 ($\omega = 2.933$). Thus, TSC1 exhibited the maximum value of electrophilicity, confirming its high capability to accept electrons.

(j) The HOMO level in the TSCN compounds was commonly localized on the C = N groups, demonstrating that they are the favored sites for Nu attack at the central metal ion.

(k) The negativity of E_{HOMO} and E_{LUMO} indicated the stability of the TSCN compounds [71].

3.2. Biological Activity

3.2.1. Antibacterial and Antifungal Activities. The antimicrobial activities of the TSCN compounds were screened. The results of the antimicrobial activities of the TSCN compounds against the tested microbes are shown in Table 3. TSC3 was inactive against the tested Gram-positive and Gram-negative bacterial species. TSC1 exhibited effective antibacterial activity against the tested bacterial strains. TSC1 exhibited an extremely higher antifungal activity against *Candida albicans* against *Amphotericin*, which is a standard antifungal agent. TSC2 exhibited moderate antibacterial activity against *Streptococcus faecalis* (Gram-positive) and *Escherichia coli* (Gram-negative). The data showed that the most effective compound was TSC1.

3.2.2. Cytotoxic Activities. The cytotoxic activity of the TSCs was investigated against liver cancer cell (HepG2) and breast cancer cell (MCF-7) lines. IC_{50} is the concentration that can diminish cancer cell growth by 50%. The results of the cytotoxic study indicated that TSC1 exhibited significant activity against the HepG2 and MCF-7 cells with IC_{50} values of 29.4 and 122 μg/mL, respectively (Table 4), while the IC_{50} values toward the HepG2 and MCF-7 cells for TSC2 were 46

Table 3: Antibacterial and antifungal activities of the synthesized thiosemicarbazone compounds.

Concentration (μg/mL)	Gram-positive			Gram-negative			Fungi	
	Bacillus subtilis	*Staphylococcus aureus*	*Streptococcus faecalis*	*E. coli*	*Neisseria gonorrhoeae*	*Pseudomonas aeruginosa*	*Aspergillus flavus*	*Candida albicans*
TSC1	14	13	17	17	12	21	0	30
TSC3	0	0	13	11	0	0	0	0
TSC4	0	0	0	0	0	0	0	0
Ampicillin	26	21	27	25	28	26	—	—
Amphotericin	—	—	—	—	—	—	16	19

Ampicillin: standard antibacterial agent, *Amphotericin*: standard antifungal agent.

Table 4: Antitumor activity of the synthesized thiosemicarbazone compounds.

Concentration (μg/mL)	TSC1	TSC2	TSC3
Liver cancer cell line (HepG2)			
5	100	100	100
25	35.3	67	22.5
50	27.4	48.7	19
IC_{50}	29.4	46	25
Breast cancer cell line (MCF-7)			
5	83.8	95	77.6
25	79.5	86.5	72
50	70.7	83	65.4
IC_{50}	122	172.9	107

and 172.9 μg/mL, respectively. Furthermore, the IC_{50} values toward the HepG2 and MCF-7 cells for TSC3 were 25 and 107 μg/mL, respectively. The antitumor results indicated that the synthesized TSCN compounds were more effective against HepG2 than MCF-7. The antitumor activity of the synthesized TSCN compounds toward HepG2 and MCF-7 cell lines followed this order: TSC3 > TSC1 > TSC2 (Figure 4).

3.2.3. Molecular Modeling and Biological Activity. Theoretical calculations were performed to investigate the physicochemical properties that possibly correlated with the antimicrobial action of the investigated TSCs. TSC1, which offered the lowest HOMO energy among the synthesized TSCs, exhibited the highest biological activity among the synthesized compounds. The data showed an inverse relationship between the dipole moment and lipophilicity, indicating that as the dipole moment decreased, the lipophilic nature of the compound increased, which powerfully favored its penetration via a lipid layer of microorganisms [72, 73], thereby violently destroying them. As shown in Table 2, the lipophilicity of TSC1 was higher than those of the other TSCN compounds, which sequentially deactivated the enzymes responsible for the respiration process of the investigated microbes more than the other compounds did, and accordingly increased its cellular uptake by bacterial cells. TSCs exhibit antibacterial activity because of the existence of toxophorically essential imine groups (–C=N) where the action mode of these compounds could include the formation of H-bonds via the azomethine group with an active center of cells that may interfere with ordinary cell processes [74].

3.3. Equilibrium Studies. The protonation constants of the TSC1 ligand were calculated (Table 5). These ligands behaved triprotic, as shown in the following equations:

$$L^- + H^+ \rightleftharpoons HL; \quad K_1 = \frac{[HL]}{[L^-][H^+]}, \tag{13}$$

$$HL + H^+ \rightleftharpoons H_2L^+; \quad K_2 = \frac{[H_2L^+]}{[HL][H^+]}, \tag{14}$$

$$H_2L^+ + H^+ \rightleftharpoons H_3L^{2+}; \quad K_3 = \frac{[HL^{2+}]}{[H^+][H_2L^+]}. \tag{15}$$

We concluded that the 1st and 2nd deprotonation constants corresponded to the deprotonation of the two N-imino sites in the TSC ligand, as shown in Scheme 3(a). The 3rd deprotonation constant corresponded to the thiolate group site in the TSC ligand, as shown in Scheme 3(b). A similar conclusion was obtained in a previous study [75].

The log $K_{N\text{-imino}}$ values ranging from 2.97 to 3.35 were similar to that observed in a previous study for the imino group (4.40) [76]. The log K_{SH} values ranging from 7.65 to 8.05 were similar to those described in a previous study for the thiolate group (5.5–9.0) [77].

A protonation equilibrium study for the TSC ligands in this study cannot be performed in an aqueous solution since it is insoluble in H_2O. The DMSO solvent has been extensively used for potentiometric studies of protonation and formation equilibria. The DMSO-water mixture (50%:50%) was best preferred to yield a soluble and stable Schiff base solution [58, 78].

Here, three protonation constants were calculated for the TSC1 ligand, and the SPECIES program was used to

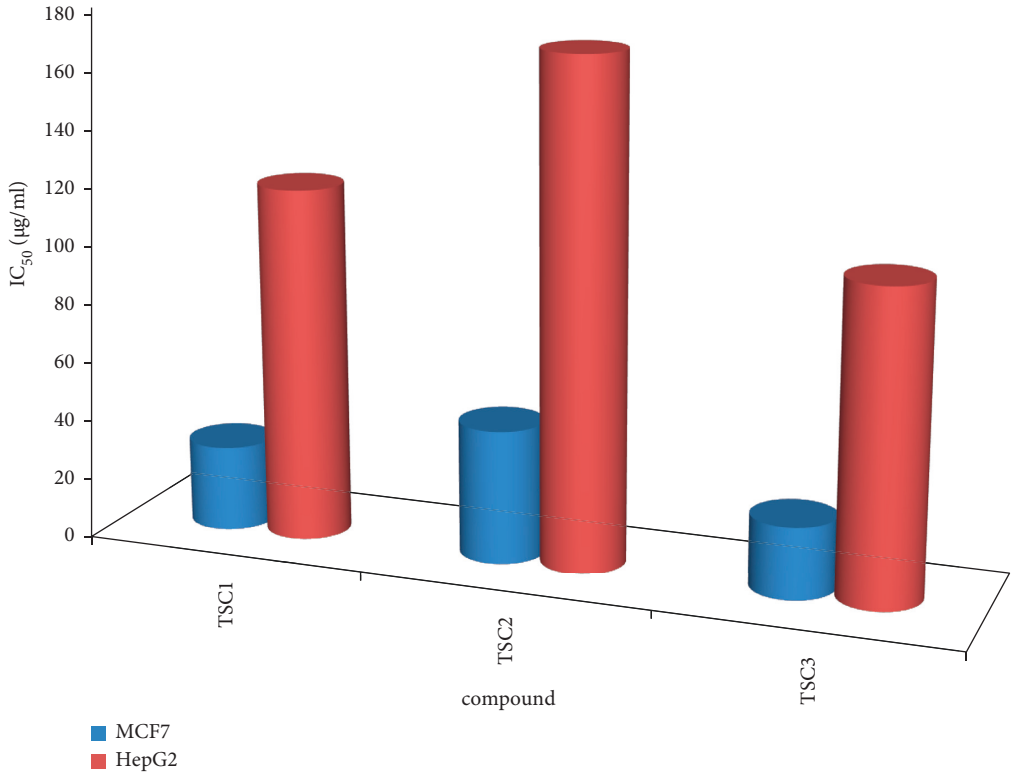

Figure 4: Cytotoxicity of TSC1, TSC2, and TSC3 on breast and liver cancer cell lines.

Table 5: Protonation constants for TSC1 ligand at different temperatures.

Reaction	log K ($\pm\sigma$)[a]		
	15°C	25°C	35°C
L + H = HL	8.02 (0.09)	7.81 (0.05)	7.64 (0.03)
HL + H = H_2L	3.31 (0.08)	3.22 (0.07)	3.14 (0.09)
H_2L + H = H_3L	3.17 (0.04)	3.08 (0.06)	3.01 (0.05)

[a](σ) is the standard deviation.

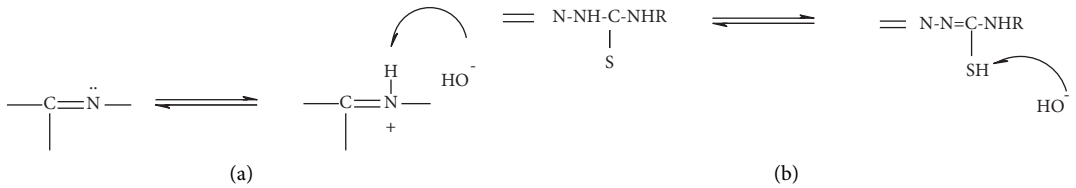

Scheme 3: (a) Possible deprotonation pathway of the imino groups and (b) possible deprotonation pathway of the thiolate group.

determine the distribution of the TSC1 ligand species as a function of pH. Figure 5(a) shows a classic species distribution diagram; it is possible to highlight, at the mentioned experimental conditions, the pH ranges within which the various species were formed and/or coexisted and their relative formation percentages. Thus, the species distribution graph is a good tool for a thorough observation of the concentration of each species present as a function of pH. It enabled us to obtain the best conditions (pH, concentration, and ligand:metal ratio) for the preparation of a solid complex. At a low pH, TSC1 initially existed in a fully protonated form with a maximum percentage of 100% as H_3L below pH < 2. Upon the addition of the base, the pH increased causing the H_3L species to lose its first proton from an imino group to form H_2L, which is the major species at a pH of 3.3. As the conditions became more alkaline, the second proton released from the second imino group began deprotonation to an HL ligand, thereby achieving the highest percent of 99.1% at a pH of 5.8. A further increase in pH was followed by the liberation of the third H^+, forming the fully deprotonated ligand, *L*, with maximum percent species of 98.4% at a pH of 10.0.

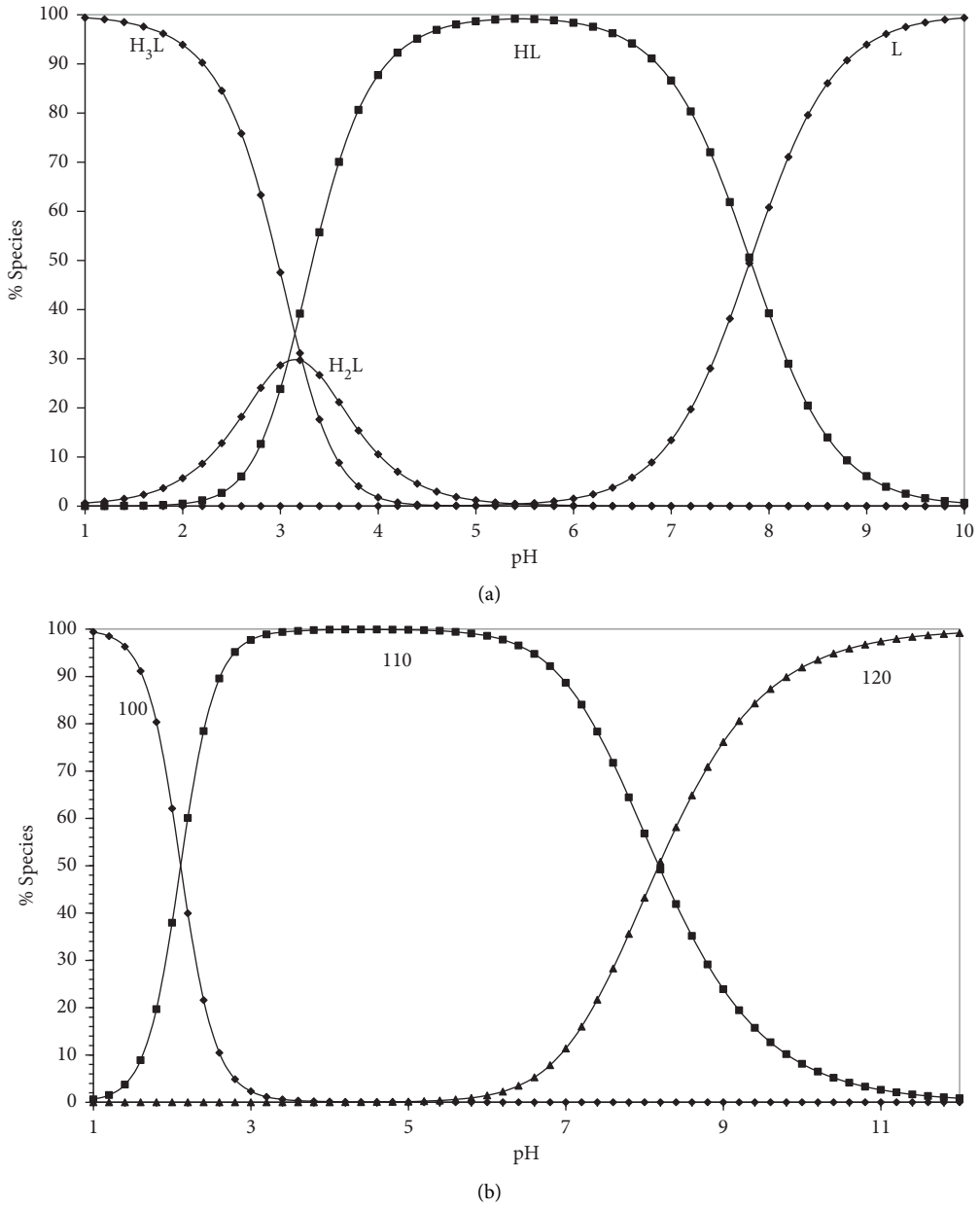

Figure 5: (a) Concentration distribution diagram of various species as a function of pH in the TSC1 system (at a concentration of TSC1 = 1.25 *mM* and $T = 25^{\circ}$C). (b) Concentration distribution diagram of various species as a function of pH in the Cd-TSC1 system.

3.3.1. Species Distribution Curves. The calculation of the equilibrium complex concentrations of Cd (II) with TSC1 (Table 6) as a function of pH showed metal (II) binding in the biological system. As an illustrative example of metal complexes, Figure 5(b) shows a concentration distribution diagram for the complex, Cd (II)-TSC1. The Cd-TSC1 complex began to form in an acidic pH range reaching a constant concentration of 99.9% at a pH of 5.0, whereas the Cd $(TSC1)_2$ complex species reached a maximum concentration of 45% at a pH of 9.8.

3.3.2. Thermodynamics. The data derived for ΔH°, ΔS°, and ΔG° related to the protonation of TSC1 and Cd (II) complex formation were calculated from the data in Tables 7 and 8. For the ligand protonation or complexation, ΔH° was determined from the plot slope (Figures 6(a)–6(b)) through the graphical representation of the Van 't Hoff equation as follows:

$$-2.303RT \log 10K = \Delta H^{\circ} - T\Delta S^{\circ},$$
$$\log K_{10} = -\left(\frac{\Delta H^{\circ}}{2.303R}\right)\left(\frac{1}{T}\right) + \frac{\Delta S^{\circ}}{R}. \quad (16)$$

With the well-known relations (6) and (7), from the ΔG and enthalpy change (ΔH) values, we calculated ΔS as follows:

Table 6: Stepwise stability for the complexes of TSC1 with Cd (II) metal ion in 50% DMSO-H_2O (V/V) solution.

Temp.(°C)	$\log K_1$ ($\pm\sigma$)[a] CdL	$\log K_2$ ($\pm\sigma$) CdL_2	$\log K_1$- $\log K_2$ Cd (II) complex
15°C	9.82(0.07)	2.80(0.03)	7.02
25°C	9.74(0.03)	2.75(0.06)	6.99
35°C	9.57(0.06)	2.71(0.09)	6.86

[a] (σ) is the standard deviation; definitions of stability constants: $K_1 = [CdL]/[Cd][L]$; $K_2 = [CdL_2]/[CdL][L]$; L = TSC1 thiosemicarbazone ligand (charges are omitted for simplicity).

Table 7: Thermodynamic parameters for the protonation of ligand (TSC1) in 50% DMSO-H_2O (V/V) solution.

Parameter[a]	Reaction								
	L + H = HL[a]			L + 2H = H_2L			L + 3H = H_3L		
	15°C	25°C	35°C	15°C	25°C	35°C	15°C	25°C	35°C
$-\Delta G$	44.25	44.59	45.08	17.49	17.58	17.82	18.26	18.38	18.47
$-\Delta H$		32.33			15.29			12.77	
ΔS		41.16			10.30			16.27	

ΔG: Gibbs energy/kJ.mol^{-1}; ΔH: enthalpy/kJ.mol^{-1}; ΔS: entropy/J.mol^{-1}.K^{-1}.

Table 8: Thermodynamic parameters for Cd (II)-TSC1 complexes in 50% DMSO-H_2O (V/V) solution.

Parameter[a]	Reaction					
	Cd + *L* = CdL			Cd + 2L = CdL_2		
	15°C	25°C	35°C	15°C	25°C	35°C
$-\Delta G$	54.18	55.60	56.45	15.45	15.70	15.99
$-\Delta H$		21.15			7.66	
ΔS		114.88			26.99	

[a]ΔG: Gibbs energy/kJ.mol^{-1}; ΔH: enthalpy/kJ.mol^{-1}; ΔS: entropy/J.mol^{-1}.K^{-1}.

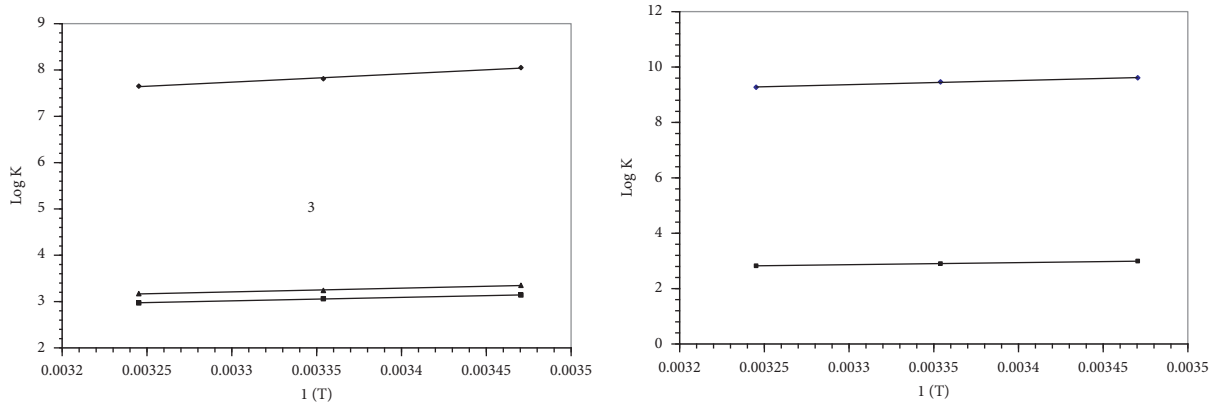

Figure 6: (a) Effect of temperature on the protonation constant of TSC1. (b) Effect of temperature on the formation constant of the Cd (II)-TSC1 complexes.

$$\Delta G^{\circ} = -2.303\,RT\log_{10}K, \tag{17}$$

$$\Delta S^{\circ} = \frac{\left(\Delta H^{\circ} - \Delta G^{\circ}\right)}{T}. \tag{18}$$

The main reasons for the protonation constant determination can be explained as follows:

(1) The ratio and pH of the various substance forms can be determined using their protonation constants.

(2) It is extremely useful in the preparation of newly synthesized compounds. The suggested structure can be reliable where protonation constants are theoretically well-calculated according to the experimental values.

(3) Considering that different types of substances exhibit different UV spectra, quantitative

spectrophotometric analyses can be performed by choosing the appropriate pH. To choose the pH, the known protonation constants are required.

(4) The preparation of buffer solutions at different pH levels requires protonation constants [43, 79].

(5) The measurements of the stability constants for the complicated formation reactions of bioactive ion compounds require protonation constants. Additionally, their protonation constants are used to calculate the stability constants of the dynamic formation of bioactive compounds with metal ions [80].

(6) The equilibrium constants of certain compounds must be understood to measure the concentration of each ionized species at a certain pH; this is fundamental to understanding their physiochemical behavior [80].

Tables 7 and 8 describe the thermodynamic functions measured and can be interpreted as follows.

(1) The corresponding thermodynamic processes for the protonation reactions include the following:

(i) Exothermic processes for neutralization reactions.

(ii) Endothermic processes for ion desolvation.

(iii) Structure alteration and alignment of H-bonds around protonated and free ligands.

(2) When the temperature increased, the value of $\log_{10} K^{H}$ decreased, and its acidity increased as the temperature increased.

(3) The negative ΔH° for the protonation of the TSC1 ligand indicated that this process was exothermic followed by the release of heat.

(4) The positive entropy of the TSC1 protonation reaction indicated increased disorder due to the desolvation processes and breakdown of H-bonds.

Table 6 lists the stepwise stability constants of the complexes formed at various temperatures. These values decreased and confirmed with an increase in temperature that the complexation phase was preferred at a low temperature.

These results provided the following findings:

(1) A negative ΔH° showed that the coordinating process was exothermic, suggesting that the metal-ligand bonds were fairly strong and that the complexity reactions were preferred at low temperatures.

(2) The complexation reactions were spontaneous with a negative ΔG°.

(3) It was widely observed that the ΔG° and ΔH° values for 1 : 1 complexes were more negative than those corresponding to 1 : 2 complexes.

(4) This can be due to the steric hindrances caused by the addition of the 2nd ligand and the principle of charge neutralization.

(5) The electrostatic attraction in the 1 : 1 complex was larger than that in 1 : 2 complex since 1 : 1 complex was formed by a dipositively charged M^{n+} and mononegatively charged ligand-anion interaction, while 1 : 2 complex was generated by a monopositively charged 1 : 1 complex and mononegatively charged ligand-anion interaction.

(6) The ΔS° values for the investigated complexes were positive, indicating that the entropy increase resultant from the release of bound solvent molecules during coordination was larger than the decrease resultant from the coordination process due to the ordered arrangement of solvent molecules around the ligand, and M^{n+} gained a random coordination pattern. This is referred to as an increase in entropy for configuration.

4. Conclusions

PTHP was condensed with thiosemicarbazide, N-ethylthiosemicarbazide, and N-phenylthiosemicarbazide in the molar ratio (1 : 1) affording the novel TSC1, TSC2, and TSC3 TSCN compounds. The novel TSCN series were characterized by different analyses. The IR spectra indicated that the TSCN compounds existed in the thione form in the solid state. TSC1 showed equipotent or even more antifungal activity when matched with the reference standard *amphotericin* reference drug against *Candida albicans*. Thus, TSC1 was considered a potential compound for extra variation as a clinically valuable antifungal agent against *Candida albicans*. The structure-activity relationship (SAR) investigation confirmed that there was an inverse relationship between the dipole moment and antimicrobial activity, which could help in the design of powerful antibacterial substances. The potentiometric studies showed that TSC1 formed complexes (1 : 1 or 1 : 2) with the Cd (II) ion. The $\log K_1$ and $-\Delta H_1$ for the Cd (II)-TSC1 TSCN complexes were to an extent larger than $\log K_2$ and $-\Delta H_2$, indicating a change in the ligand dentate character from the tridentate (SNN donors) in 1 : 1 chelates to the bidentate (SN-donors) in 1 : 2; M:L chelates in addition to the steric hindrance generated by the entry of the 2nd molecule. The coordination of Cd (II) to TSC1 was spontaneous, exothermic, and entropically favorable. The molecular properties of the synthesized TSCN compounds were investigated by DFT calculations. These compounds may be considered a good remedy for Cd^{2+} ion toxicity because they formed a highly stable complex with it. The variation in the substitution of the N-thiosemicarbazide moiety was considered vital for the functionalization of the synthesized compounds, owing to its significance in the inhibition process.

Data Availability

The CIF report and spectral data used to support the findings and structures in this study are included within the supplementary files.

Disclosure

A preprint has previously been published at Research Square.

Conflicts of Interest

The authors declare that they have no conflicts of interest.

Acknowledgments

The authors express gratitude to the Europe PMC for their help in citing the early view of the manuscript [81, 82].

Supplementary Materials

The structures of TSC2 and TSC3 were established through X-ray crystallography. CCDC 2026108 and CCDC 2033322 contain the supplementary crystallographic data for these two compounds. (*Supplementary Materials*)

References

[1] World health statistics, *WHO Library Cataloguing-in-Publication Data*, WHO, Geneva, Switzerland, 2014.

[2] A. Anandan, G. L. Evans, K. Condic-Jurkic et al., "Structure of a lipid A phosphoethanolamine transferase suggests how conformational changes govern substrate binding," *Proceedings of the National Academy of Sciences*, vol. 114, no. 9, pp. 2218–2223, 2017.

[3] H. Harbottle, S. Thakur, S. Zhao, and D. G. White, "Genetics of antimicrobial resistance," *Animal Biotechnology*, vol. 17, no. 2, pp. 111–124, 2006.

[4] B. Li and T. J. Webster, "Bacteria antibiotic resistance: new challenges and opportunities for implant-associated orthopedic infections," *Journal of Orthopaedic Research: official Publication of the Orthopaedic Research Society*, vol. 36, no. 1, pp. 22–32, 2018.

[5] S. Berger, "Incidence of severe side effects during therapy with sulphonylurea and biguanides," *Hormone and Metabolic Research*, vol. 17, pp. 111–115, 1985.

[6] B. Lakshmi, P. G. Avaji, K. N. Shivananda, P. Nagella, S. H. Manohar, and K. N. Mahendra, "Synthesis, spectral characterization and *in vitro* microbiological evaluation of novel glyoxal, biacetyl and benzil bis-hydrazone macrocyclic Schiff bases and their Co (II), Ni (II) and Cu (II) complexes," *Polyhedron*, vol. 30, no. 9, pp. 1507–1515, 2011.

[7] J. Chan, Y. Huang, G. Liu et al., "The cytotoxicity and mechanisms of 1,2-naphthoquinone thiosemicarbazone and its metal derivatives against MCF-7 human breast cancer cells," *Toxicology and Applied Pharmacology*, vol. 197, pp. 40–48, 2004.

[8] K. J. Duffy, A. N. Shaw, E. Delorme et al., "Identification of a pharmacophore for thrombopoietic activity of small, non-peptidyl molecules. 1. Discovery and optimization of salicylaldehyde thiosemicarbazone thrombopoietin mimics," *Journal of Medicinal Chemistry*, vol. 45, no. 17, pp. 3573–3575, 2002.

[9] J. R. Dilworth and R. Hueting, "Metal complexes of thiosemicarbazones for imaging and therapy," *Inorganica Chimica Acta*, vol. 389, pp. 3–15, 2012.

[10] S. A. Andres, K. Bajaj, N. S. Vishnosky et al., "Synthesis, characterization, and biological activity of hybrid thiosemicarbazone-alkylthiocarbamate metal complexes," *Inorganic Chemistry*, vol. 59, no. 7, pp. 4924–4935, 2020.

[11] P. Heffeter, V. F. S. Pape, E. V. A. Enyedy, B. K. Keppler, G. Szakacs, and C. R. Kowo, "Anticancer thiosemicarbazones: chemical properties, interaction with iron metabolism, and resistance development," *Antioxidants and Redox Signaling*, vol. 30, no. 8, p. 7487, 2017.

[12] R. J. Glisoni, M. L. Cuestas, V. L. Mathet, J. R. Oubiña, A. G. Moglioni, and A. Sosnik, "Antiviral activity against the hepatitis C virus (HCV) of 1-indanone thiosemicarbazones and their inclusion complexes with hydroxypropyl-β-cyclodextrin," *European Journal of Pharmaceutical Sciences*, vol. 47, no. 3, pp. 596–603, 2012.

[13] R. MendozMeroño, L. Menendez-Taboada, and S. García-Granda, "1-(4-Carb-oxy-butan-2-yl-idene)-4-phenyl-thiosemicarbazide," *Acta Crystallographica, Section E: Structure Reports Online*, vol. 68, pp. o1945–6, 2012.

[14] A. Ma, H. C. Kwong, and F. Adam, "The crystal structure of ((cyclo-hexyl-amino) {(Z)-2-((E)-5-meth-oxy-3-nitro-2-oxido-benzyl-idene-κO) hydrazin-1-yl-idene-κN2} methane-thiol-ato-κS) (dimethyl sulfoxide-κS) platinum (II): a supramolecular two-dimensional network," *Acta Crystallogr E Crystallogr Commun*, vol. 75, pp. 1486–1489, 2019.

[15] J. P. Scovill, D. L. Klayman, and D. G. Franchino, "2-Acetylpyridine thiosemicarbazones. 4. Complexes with transition metals as antimalarial and antileukemic agents," *Journal of Medicinal Chemistry*, vol. 25, no. 10, pp. 1261–1264, 1982.

[16] L. Klayman, J. P. Scovill, J. F. Bartosevich, and J. Bruce, "2-Acetylpyridine thiosemicarbazones. 5. 1-(1-(2-Pyridyl)ethyl)-3-thiosemicarbazides as potential antimalarial agents," *Journal of Medicinal Chemistry*, vol. 26, no. 1, pp. 35–39, 1983.

[17] K. Anđelković, D. Sladić, A. Bacchi, G. Pelizzi, N. Filipović, and M. Rajković, "Complexes of iron (II), iron (III) and zinc (II) with condensation derivatives of 2-acetylpyridine and oxalic or malonic dihydrazide. Crystal structure of tris ((1-(2-pyridyl) ethylidene) hydrazine) iron (II) perchlorate," *Transition Metal Chemistry*, vol. 30, pp. 243–250, 2005.

[18] P. K. Singh and D. N. Kumar, "Spectral studies on cobalt (II), nickel (II) and copper (II) complexes of naphthaldehyde substituted aroylhydrazones," *Spectrochimica Acta Part A: Molecular and Biomolecular Spectroscopy*, vol. 64, no. 4, pp. 853–858, 2006.

[19] N. Bharti, S. S. Shailendra, A. Sharma, F. Naqvi, and A. Azam, "New palladium (II) complexes of 5-nitrothiophene-2-carboxaldehyde thiosemicarbazones," *Bioorganic & Medicinal Chemistry*, vol. 11, no. 13, pp. 2923–2929, 2003.

[20] A. Walcourt, M. Loyevsky, D. B. Lovejoy, V. R. Gordeuk, and D. R. Richardson, "Novel aroylhydrazone and thiosemicarbazone iron chelators with anti-malarial activity against chloroquine-resistant and -sensitive parasites," *Journal of Biochemistry & Cell Biology*, vol. 36, 2004.

[21] O. M. I. Adly and A. A. A. Emara, "Spectroscopic and biological studies of new binuclear metal complexes of a tridentate ONS hydrazone ligand derived from 4-amino-6-methyl-3-thioxo-3,4-dihydro-1,2,4-triazin-5(2H)-one and 4,6-diacetylresorcinol," *Spectrochimica Acta Part A: Molecular and Biomolecular Spectroscopy*, vol. 132, pp. 91–101, 2014.

[22] O. A. El-Gammal, T. H. Rakha, H. M. Metwally, and G. M. Abu El-Reash, "Synthesis, characterization, DFT and biological studies of isatinpicolinohydrazone and its Zn (II), Cd (II) and Hg (II) complexes," *Spectrochimica Acta Part A: Molecular and Biomolecular Spectroscopy*, vol. 127, pp. 144–156, 2014.

[23] R. Kaplánek, M. Havlík, B. Dolenský et al., "Synthesis and biological activity evaluation of hydrazone derivatives based on a Tröger's base skeleton," *Bioorganic & Medicinal Chemistry*, vol. 23, no. 7, pp. 1651–1659, 2015.

[24] M. M. Moniuszko-Jakoniuk and J. Moniusko-Jakoniuk, "Interactions between cadmium and zinc in the organism," *Food and Chemical Toxicology*, vol. 39, no. 10, pp. 967–980, 2001.

[25] I. M. Armitage, A. J. M. Schoot Viterkamp, J. R. Chlebowski, and J. E. Coleman, "^{113}Cd NMR as a probe of the active sites of metalloenzymes," *Journal of Magnetic Resonance*, vol. 29, pp. 375–392, 1978.

[26] H. Beinert, "Structure and function of copper proteins report, on the fourth La cura conference held at villa giulia, manziana, rome, Italy, 4-8 september 1979," *Coordination Chemistry Reviews*, vol. 33, no. 1, pp. 55–85, 1980.

[27] F. Jensen, *Introduction to Computational Chemistry*, Wiley, Chichester, UK, 1999.

[28] Y. D. Scherson, S. J. Aboud, J. Wilcox, and B. J. Cantwell, "Surface structure and reactivity of rhodium oxide," *Journal of Physical Chemistry C*, vol. 115, no. 22, 2011.

[29] A. A. El-Sherif, "Coordination properties of bidentate (N,O) and tridentate (N,O,O) heterocyclic alcohols with dimethyltin (IV)," *Journal of Coordination Chemistry*, vol. 64, no. 7, pp. 1240–1253, 2011.

[30] A. A. El-Sherif, "Potentiometric determination of the stability constants of trimethyltin (IV) chloride complexes with imino-bis (methylphosphonic acid) in water and dioxane-water mixtures," *Journal of Solution Chemistry*, vol. 41, no. 3, pp. 392–409, 2012.

[31] N. Rabjohn, *Organic Synthesis, Collective*, John Wiley & Sons, Hoboken, NJ, USA, 1963.

[32] A. A. El-Sherif, "Synthesis, spectroscopic characterization and biological activity on newly synthesized copper (II) and nickel (II) complexes incorporating bidentate oxygen-nitrogen hydrazone ligands," *Inorganica Chimica Acta*, vol. 362, no. 14, pp. 4991–5000, 2009.

[33] A. Altomare, G. Cascarano, C. Giacovazzo et al., "SIR92 - a program for automatic solution of crystal structures by direct methods," *Journal of Applied Crystallography*, vol. 27, no. 3, p. 435, 1994.

[34] S. Mackay, C. J. Gilmore, C. Edwards, N. Stewart, and K. Shankland, *maXus, Computer Program for the Solution and Refinement of Crystal Structures*, The University of Glasgow, Glasgow, Scotland, 1999.

[35] C. K. Johnson, *ORTEP-II. A Fortran Thermal-Ellipsoid Plot Program. Report ORNL-5138*, Oak Ridge National Laboratory, Oak Ridge, TN, USA, 1976.

[36] A. A. El-Sherif, "Mixed ligand complex formation reactions and equilibrium studies of Cu (II) with bidentate heterocyclic alcohol (N, O) and some bio-relevant ligands," *Journal of Solution Chemistry*, vol. 39, no. 1, pp. 131–150, 2010.

[37] R. G. Bates, *Determination of pH, Theory and Practice*, John Wiley & Sons, Hoboken, NJ, USA, 2nd edition, 1975.

[38] E. M. Woolley, D. G. Hurkot, and L. G. Hepler, "Ionization constants for water in aqueous organic mixtures," *Journal of Physical Chemistry*, vol. 74, pp. 3908–3913, 1970.

[39] G. L. Van Uitert and C. G. Hass, "Studies on the coordination compounds," *Journal of the American Chemical Society*, vol. 75, p. 451, 1971.

[40] E. P. Serjeant, *Potentiometry and Potentiometric Titrations*, Wiley, Hoboken, NJ, USA, 1984.

[41] A. Golcu, M. Tumer, H. Demirelli, and R. A. Wheatley, "Cd (II) and Cu (II) complexes of polydentate Schiff base ligands: synthesis, characterization, properties and biological activity," *Inorganica Chimica Acta*, vol. 358, no. 6, pp. 1785–1797, 2005.

[42] A. E. Martell and R. J. Motekaitis, *The Determination and Use of Stability Constants*, VCH, Vancouver, Canada, 1988.

[43] M. Meloun, J. Havel, and E. Högfelt, *Computation of Solution Equilibria: A Guide to Methods in Potentiometry, Extraction and Spectrophotometry*, Wiley, Hoboken, NJ, USA, 1988.

[44] P. Gans, A. Sabatini, and A. Vacca, "An improved computer program for the computation of formation constants from potentiometric data," *Inorganica Chimica Acta*, vol. 18, pp. 237–239, 1976.

[45] L. Pettit, *Personal Communication*, University of Leeds, Leeds, UK, 1984.

[46] B. A. Delley, "A scattering theoretic approach to scalar relativistic corrections on bonding," *International Journal of Quantum Chemistry*, vol. 69, no. 3, pp. 423–433, 1998.

[47] B. Delley, "From molecules to solids with the DMol3 approach," *The Journal of Chemical Physics*, vol. 113, no. 18, pp. 7756–7764, 2000.

[48] *Materials Studio (Version 5.0)*, Accelrys software Inc, San Diego, CA, USA, 2009.

[49] W. J. Hehre, L. Radom, P. V. R. Schlyer, and J. A. Pople, *Ab Initio Molecular Orbital Theory*, Wiley, Hoboken, NJ, USA, 1986.

[50] B. Hammer, L. B. Hansen, and J. K. Nørskov, "Improved adsorption energetics within density-functional theory using revised Perdew-Burke-Ernzerhof functionals," *Physical Review B*, vol. 59, no. 11, pp. 7413–7421, 1999.

[51] A. Matveev, M. Staufer, M. Mayer, and N. Rosch, "Density functional study of small molecules and transition-metal carbonyls using revised PBE functionals," *International Journal of Quantum Chemistry*, vol. 75, no. 4-5, pp. 863–873, 1999.

[52] A. W. Bauer, W. M. M. Sherris, J. C. Turck, and M. Turck, "Antibiotic susceptibility testing by a standardized single disk method," *American Journal of Clinical Pathology*, vol. 45, no. 4, pp. 493–496, 1966.

[53] A. A. El-Sherif, "Synthesis, solution equilibria and antibacterial activity of Co (II) with 2-(aminomethyl)-benzimidazole and dicarboxylic acids," *Journal of Solution Chemistry*, vol. 39, no. 10, pp. 1562–1581, 2010.

[54] P. Skehan, R. Storeng, D. Scudiero et al., "New colorimetric cytotoxicity assay for anticancer-drug screening," *JNCI Journal of the National Cancer Institute*, vol. 82, no. 13, pp. 1107–1112, 1990.

[55] National Committee for Clinical Laboratory Standards, *Methods for Dilution Antimicrobial Susceptibility Tests for Bacteria that Grow Aerobically*, Approved Standard M7-A3, Villanova, PA, USA, 1993.

[56] M. R. P. Kurup and M. S. Joseph, "Synthesis and reactivity in inorganic and metal-organic chemistry," *Inorganic and Metal-Organic Chemistry*, vol. 33, pp. 275–281, 2003.

[57] D. M. Wileasn and D. T. Suprunchuk, "The infrared absorption spectra of thiosemicarbazide and related compounds: NH_2 and NH vibrations," *Canadian Journal of Chemistry*, vol. 47, pp. 1087–1089, 1969.

[58] M. Aljahdali and A. A. El-Sherif, "Synthesis, characterization, molecular modeling and biological activity of mixed ligand complexes of Cu (II), Ni (II) and Co (II) based on 1,10-phenanthroline and novel thiosemicarbazone," *Inorganica Chimica Acta*, vol. 407, pp. 58–68, 2013.

[59] V. Philip, V. Suni, M. R. P. Prathapachandra Kurup, and M. Nethaji, "Copper (II) complexes derived from di-2-pyridyl ketone N (4), N (4)-(butane-1,4-diyl) thiosemicarbazone:

crystal structure and spectral studies," *Polyhedron*, vol. 25, no. 9, pp. 1931–1938, 2006.

[60] R. G. Pearson, "Absolute electronegativity and hardness: applications to organic chemistry," *Journal of Organic Chemistry*, vol. 54, no. 6, pp. 1423–1430, 1989.

[61] P. Geerlings, F. De Proft, and W. Langenaeker, "Conceptual density functional theory," *Chemical Reviews*, vol. 103, no. 5, pp. 1793–1874, 2003.

[62] R. G. Parr, L. V. Szentpály, and S. Liu, "Electrophilicity index," *Journal of the American Chemical Society*, vol. 121, no. 9, pp. 1922–1924, 1999.

[63] P. K. Chattaraj and S. Giri, "Electrophilicity index within a conceptual DFT framework," *Annual Reports Section "C" (Physical Chemistry)*, vol. 105, pp. 13–39, 2009.

[64] G. Speie, J. Csihony, A. M. Whalen, and C. G. Pie-Pont, "The synthesis, spectroscopy, and structure of three Cu (II) co-ordination compounds of the ligands bis (imidazole-2-yl) methylaminomethane," *Inorganic Chemistry*, vol. 35, p. 3519, 1996.

[65] G. Huang, X. Zhang, Y. Fan et al., "Synthesis, crystal structure and theoretical calculation of a novel nickel (II) complex with dibromotyrosine and 1,10-phenanthroline," *Bulletin of the Korean Chemical Society*, vol. 34, no. 10, pp. 2889–2894, 2013.

[66] S. Sagdinc, B. Köksoy, F. Kandemirli, and S. H. Bayari, "Theoretical and spectroscopic studies of 5-fluoro-isatin-3-(N-benzylthiosemicarbazone) and its zinc (II) complex," *Journal of Molecular Structure*, vol. 917, no. 2-3, pp. 63–70, 2009.

[67] R. G. Pearson, *Hard and Soft Acids and Bases*, Dowden, Hutchinson and Ross, Stroudsburg, 1973.

[68] K. H. Kim, Y. K. Han, and J. Jung, "Basis set effects on relative energies and HOMO-LUMO energy gaps of fullerene C36," *Theoretical Chemistry Accounts*, vol. 113, no. 4, pp. 233–237, 2005.

[69] A. Ghosh, A. Sarkar, P. Mitra et al., "Crystal structure and DFT calculations of 3,4-seco-lup-20 (29)-en-3-oic acid isolated from Wrightia tinctoria: stacking of supramolecular dimers in the crystal lattice," *Journal of Molecular Structure*, vol. 980, no. 1-3, pp. 7–12, 2010.

[70] J. I. Aihara, "Reduced HOMO–LUMO gap as an index of kinetic stability for polycyclic aromatic hydrocarbons," *The Journal of Physical Chemistry A*, vol. 103, no. 37, pp. 7487–7495, 1999.

[71] G. A. Al-Hazmi, K. S. Abou-Melha, N. M. El-Metwaly, and K. A. Saleh, "Synthesis of novel vo (ii)-perimidine complexes: spectral, computational, and antitumor studies," *Bioinorganic Chemistry and Applications*, vol. 2018, Article ID 7176040, 22 pages, 2018.

[72] A. T. Abdelkarim, "Potentiometric, thermodynamics and coordination properties for binary and mixed ligand complexes of copper (II) with cephradine antibiotic and some N- and O-bound amino acids (α-alanine and β-alanine)," *Journal of Molecular Liquids*, vol. 328, Article ID 115334, 2021.

[73] C. Jayabalakrishnan and K. Natarjan, "Synthesis of copper (II) and nickel (II) complexes using compartmental ligands: X-ray, electrochemical and magnetic studies," *Polyhydron*, vol. 20, pp. 3039–3048, 2001.

[74] A. A. El-Sherif and M. M. Shoukry, "Ternary copper (II) complexes involving 2-(aminomethyl)-benzimidazole and some bio-relevant ligands. Equilibrium studies and kinetics of hydrolysis for glycine methyl ester under complex formation," *Inorganica Chimica Acta*, vol. 360, no. 2, pp. 473–487, 2007.

[75] M. Metwally, S. Bondock, H. El-Azap, and E. Kandeel, "Thiosemicarbazides: synthesis and reactions," *Journal of Sulfur Chemistry*, vol. 32, no. 5, pp. 489–519, 2011.

[76] T. Gündüz, E. Kiliç, F. Köseo, and E. Canel, "Protonation constants of some substituted salicylideneanilines in dioxan-water mixtures," *Analytica Chimica Acta*, vol. 282, no. 3, pp. 489–495, 1993.

[77] F. G. Bordwell and D. L. Hughes, "Thiol acidities and thiolate ion reactivities toward butyl chloride in dimethyl sulfoxide solution. the question of curvature in Broensted plots," *Journal of Organic Chemistry*, vol. 47, no. 17, pp. 3224–3232, 1982.

[78] A. A. El-Sherif, M. M. Shoukry, and M. M. A. Abd-Elgawad, "Protonation equilibria of some selected α-amino acids in DMSO-water mixture and their Cu (II)-Complexes," *Journal of Solution Chemistry*, vol. 42, no. 2, pp. 412–427, 2013.

[79] H. Rossotti, *The Study of Ionic Equilibria*, Longman, London, UK, 1987.

[80] H. Sigel and R. B. Martin, "Coordinating properties of the amide bond. Stability and structure of metal ion complexes of peptides and related ligands," *Chemical Reviews*, vol. 82, no. 4, pp. 385–426, 1982.

[81] "Pre-print in research square," https://www.researchsquare.com/article/rs-647955/v1.

[82] "Europe PMC," https://europepmc.org/article/ppr/ppr364288.